Improvement of ^{93m}Nb and ^{103m}Rh activity measurement methodology for reactor dosimetry

J. Riffaud[1,a], M.-C. Lépy[1], C. Domergue[2], H. Philibert[2], C. Destouches[2], N. Thiollay[2], J.M. Girard[2]

[1]*CEA, LIST, Laboratoire National Henri Becquerel (LNE-LNHB), CEA-Saclay, Bât 602, PC 111, 91191 Gif-sur-Yvette CEDEX, France*
[2]*CEA, DEN, DER, Laboratoire de Dosimétrie, Capteurs et Instrumentation (LDCI), Cadarache, 13108 Saint Paul-lez-Durance, France*

Abstract. Reactor dosimetry is based on the analysis of the activity of irradiated dosimeters, such as ^{93m}Nb and ^{103m}Rh. The activity measurement of these dosimeters is conventionally performed by X-ray spectrometry, but the low-energy of emitted photons makes it difficult to derive reliable results with low uncertainties. Approaches to improve these characterisations are presented: they include high accuracy efficiency calibration of a HPGe detector using both experiments and Monte Carlo simulation, calculation of corrective factors for the geometry (self-absorption) and self-fluorescence effects. Improvement of the knowledge of the ^{103m}Rh decay scheme is also required and a specific experiment is proposed, including activity measurement of a ^{103m}Rh solution by liquid scintillation, and measurement of the photon emission intensities by X-ray spectrometry. A method for calculating coefficients to take into account the self-fluorescence effects in dosimeters is also suggested to improve the uncertainties on activity measurements.

1. Introduction

Reactor dosimetry aims at determining the neutron flux density received during an irradiation and to characterise the energy distribution of neutrons. This technique is based on the analysis of the activity of irradiated dosimeters including isotopes which are subject to activation or fission reactions under the neutron flux. For example, inelastic scattering reactions (n, n') are useful to characterise neutron beams with energies around 1 MeV [1-4]. Both reactions ^{93}Nb(n,n')^{93m}Nb and ^{103}Rh(n,n')^{103m}Rh are of particular importance for dosimetry in reactor. The measurement of the activity of Nb and Rh dosimeters provides the basic data that can be traced back to the reactor operating information.

The activity measurement of such dosimeters is conventionally performed by X-ray spectrometry. Unfortunately, the low-energy of emitted photons makes it difficult to derive results with sufficiently low uncertainties. Indeed, the efficiency calibration of the detector must be accurately performed and self-attenuation in the dosimeter must be taken into account. In addition, niobium and rhodium are not 100 % pure, other elements are present. These impurities and other isotopes of niobium and rhodium created during irradiation are activated by neutrons and induce fluorescence in the dosimeters which increase their activity. In the present study, different aspects of the methodology used to measure the dosimeters activity are examined and improvements of the usual measurement procedure are provided.

2. ^{93m}Nb and ^{103m}Rh decay schemes

Activation of niobium dosimeters produces ^{93m}Nb, characterised with a half-life of 16.12 (15) years, which decays by gamma transition to the ground state of the stable nuclide ^{93}Nb (Figure1 – left panel). This transition is highly converted thus leading to the emission of characteristic X-rays of niobium, with energies for K X-rays between 16.5 keV and 19 keV. Their emission intensities are quoted with relative standard uncertainties of the order of 2% [5].

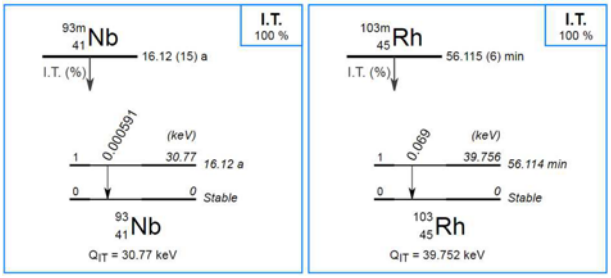

Fig. 1. Decay scheme of ^{93m}Nb (left) and ^{103m}Rh (right) [5]

The decay scheme of ^{103m}Rh is similar to that of ^{93m}Nb (Figure1 – right panel). Its half-life is short (56.115 (6) minutes) and the transition from the isomeric state to the ground state of ^{103}Rh is highly converted, resulting in X-ray emissions, with energies for K transitions between 20 keV and 23.2 keV. The emission intensities of the K X-rays are specified with relative standard uncertainties between 5.5 and 7% [6].

[a] Corresponding author: jonathan.riffaud@cea.fr

3. X-ray spectrometry

3.1 Efficiency calibration

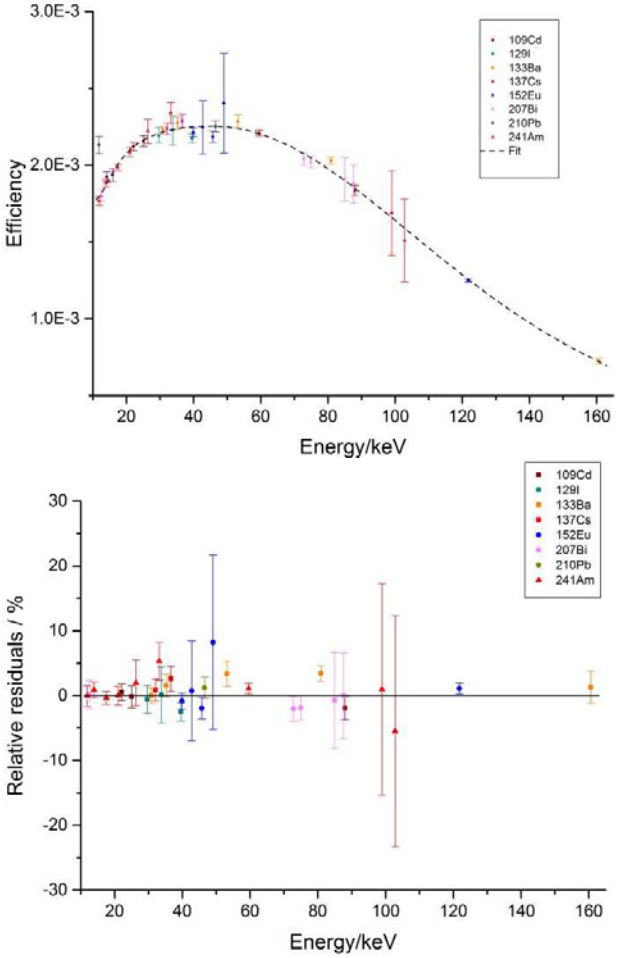

Fig. 2. Experimental efficiency calibration: experimental values and fitted curve. The lower panel displays relative residuals.

X-ray spectrometry is performed using a high-purity germanium (HPGe) detector. The experimental efficiency calibration is defined for a reference geometry, using radioactive standard point sources for a given source-detector distance (8 cm). The radionuclides used are ^{88}Y, ^{109}Cd, ^{133}Ba, ^{137}Cs, ^{152}Eu, ^{207}Bi, ^{210}Pb and ^{241}Am. The radioactive solutions are standardised at the Laboratoire National Henri Becquerel by absolute methods with relative combined uncertainties less than 1%. Then a weighted drop of solution is deposited between two sheets of Mylar® to prepare point sources for γ- and X-ray spectrometry. These are used to establish the full-energy peak efficiency calibration of HPGe detectors, according to:

$$\varepsilon(E) = \frac{N(E)}{A\, I(E)\, t} \prod_i C_i \qquad (1)$$

Where ε(E) is the detection efficiency at the energy "*E*", *N(E)* is the number of counts under the full-energy peak with energy "*E*", *A* the activity of the radionuclide included in the standard point source, *I(E)* the emission intensity line with energy line "*E*", *t* the acquisition time and C_i stands for different correction factors.
The experimental values are fitted using least-square method, to have an efficiency value for any energy, with the use of a poly-logarithmic function (Figure 2). Both experimental and efficiency values are obtained with 1.5 % relative combined standard uncertainties.

3.2 Efficiency calculation with Monte Carlo method

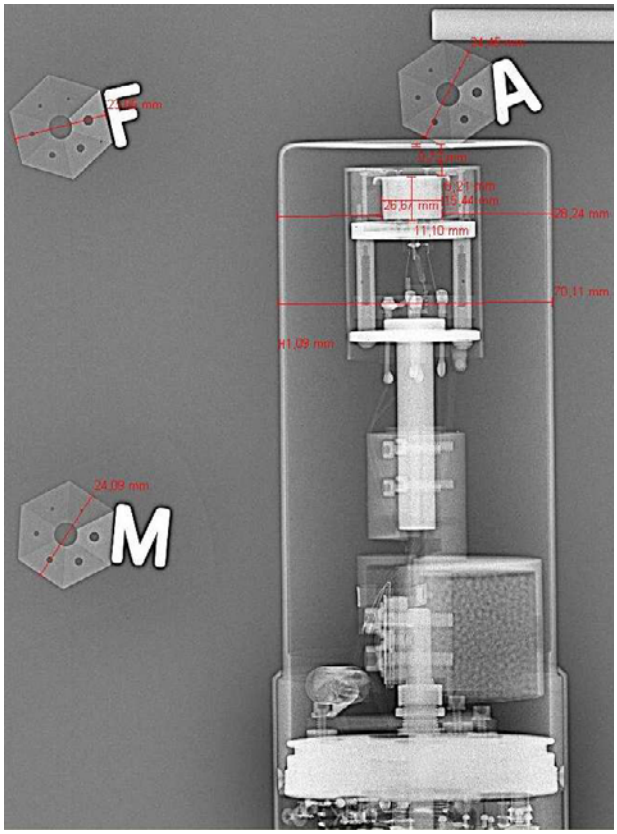

Fig. 3. Radiography of the detector

Due to the poor knowledge of the photon emission intensities of radionuclides in the low energy range, the efficiency calibration curve was refined using Monte Carlo simulation. PENELOPE [7] and GEANT4 [8] code were used and optimisation of physical parameters of the germanium crystal was necessary to adjust the efficiency curve obtained with the simulation with the experimental fit. We started with the dimensions provided by the manufacturer and those which can be determined from the radiography of the detector (Figure 3). The result (Figure 4) was obtained after many changes in the crystal dimensions with relative differences between experimental and simulations lower than 1%. The results obtain with GEANT4 are very close to those of PENELOPE, the low-energy models used with GEANT4 is the PENELOPE physics package.

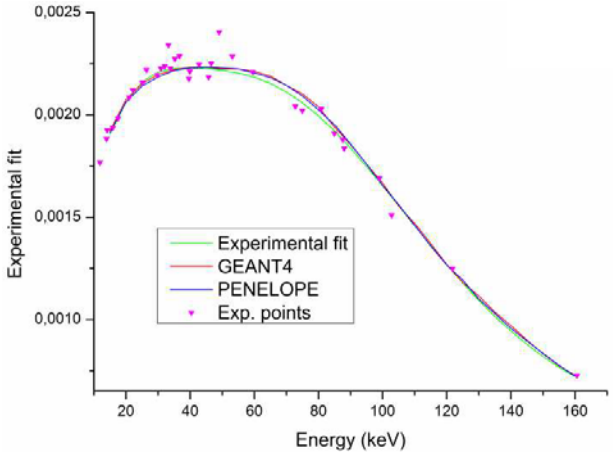

Fig. 4. Efficiency of the spectrometer as a function of photon energy. The experimental efficiency curve is shown by the green curve and the Monte Carlo computed efficiency by the red curve with the use of GEANT4 code and the blue curve with PENELOPE code.

4 Measurement procedures

4.1 ^{93m}Nb

The dosimeter activity measurement is carried out using the calibrated HPGe detector, at the same distance than the reference point sources. The activity measurement, *A*, is obtained from the number of counts under the full-energy peaks of K X-rays, and calculated with the following formula:

$$A = \frac{N(E)}{I(E)\,\varepsilon(E)\,t}\prod_i C_i \qquad (2)$$

In addition to corrections for radionuclide decay and coincidence summing, such as used for the efficiency calibration, further specific corrections must be taken into account to obtain the activity of the dosimeters. The sample is in the shape of a metal strip, 5 mm long, 1 mm wide and 19.89 µm thick. Corrective factors must be applied to take into account the change in geometry and self-absorption of X-rays in the material thickness.
Self-absorption and geometry corrections are computed by Monte Carlo simulation. In spite of the thinness of the dosimeter (20 µm) the self-absorption correction is around 20%. Currently, the relative standard uncertainty on activity measurement is about 6%. Correction coefficients for fluorescence caused by each impurity were calculated in 1972. The value of these corrections depends on the activity of the impurities compared to the activity of the dosimeter and can vary from 0.5% to 7%. The activity of the impurities is measuresd by classical γ-ray spectrometry.

4.2 ^{103m}Rh

The measurement activity procedure for reactor dosimetry is the same as in the case of ^{93m}Nb; however, these are pellets of pure ^{103}Rh which are irradiated. But uncertainties on the X-ray intensities lead to high uncertainties in measurement results, of the order of 10%. Self-absorption and geometry corrections are taken into account and computed as for ^{93m}Nb. With a thickness of 50 µm, the self-absorption in rhodium dosimeters is about 50%. The correction coefficients for fluorescence have never been calculated for rhodium impurities. Because, unlike the niobium, only the fluorescence induced by iridium impurities can disturb the measurements, and should be considered.

5 Improvement of decay data

Emission intensities of X-rays in the recommended data for isomeric transition are determined from the γ-ray transition probabilities, internal conversion coefficients and fluorescence yield values [9]. The knowledge of the fluorescence yields for ^{93m}Nb is rather poor and based on old experiments [10]. All data for ^{103m}Rh, are not well known and leading to high uncertainties on emission intensities [10]. Two experiments were performed to measure the K fluorescence yields of Nb and Rh and the emission intensities of K X-rays of ^{103m}Rh, in order to improve the knowledge of the decay data.

5.1 K fluorescence yields measurements

New measurements of the K fluorescence yields of niobium and rhodium were performed, taking advantage of optimized experimental facilities, using tunable monochromatic X-rays [10]. The experiment included two steps:

5.1.1 Mass attenuation coefficients

First, accurate values of the mass attenuation coefficients $(\frac{\mu}{\rho}(E))$ of niobium and rhodium were measured at the SOLEIL synchrotron [11]. These coefficients were obtained following an experimental procedure previously established and validated for similar measurements on different metallic targets [12,13]. Mass attenuation coefficients, were measured in transmission mode using a monochromatic parallel photon beam with energy *E*, under normal incidence to the sample with thickness *x*. The measurement consists in measuring the intensity of a monochromatic photon flux in front the sample, $I_0(E)$, and immediately behind it $I(E)$. For each energy step, the mass attenuation coefficient can be calculated assuming the Beer-Lambert law:

$$I(E) = I_0(E)\, e^{-\frac{\mu}{\rho}(E)\rho x} \qquad (3)$$

where μ is the linear attenuation coefficient of the target material and ρ is the material density.

5.1.2 Fluorescence yields

In the second step, the fluorescence yields are measured in a reflection mode (Figure 5) where the target (niobium or rhodium) is placed at the angle of 45° relative to the incident monochromatic photon beam, with energy E_0 and intensity I_0. Electronic rearrangement following

photoelectric effect induces X-ray emission with energy *Ei* according to the partial K fluorescence yield ω_{Ki}. These are recorded with an energy-dispersive detector (HPGe) installed at 45° from the target. Thus, the full-energy peak areas of each line, Ni, allow deriving the partial fluorescence yield, according to:

$$\omega_{Ki} = \frac{4\pi}{\Omega}\frac{N_i}{\varepsilon_i}\frac{1}{I_0\tau_K}\frac{\mu_0+\mu_i}{1-e^{-\frac{\mu_0+\mu_i}{\sin\frac{\pi}{4}}l}} \quad (4)$$

Where:

Ω : detection solid angle,

ε_i: full-energy peak (FEP) efficiency of the HPGe detector,

τ_K : photoelectric interaction cross section in the K shell

μ_0 and μ_i : mass attenuation coefficients of the target material for the incident and the emitted photon beams, respectively.

Using nine incident energies ranging from 20 keV to 25 keV, the total K fluorescence yield for niobium was obtained as ω_K= 0.724 (14). For rhodium, results were derived with an average of eight measurements with incident photons in the 26 keV to 30 keV energy range. The total K fluorescence yield of rhodium was computed as ω_K= 0.814 (41).

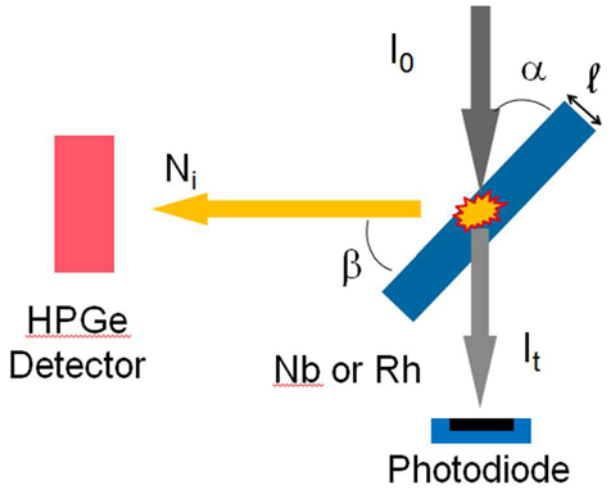

Fig. 5. Geometry of the experimental setup for fluorescence yields measurements

5.2 Photon emission intensities of ^{103m}Rh

A specific experiment was planned in order to measure the absolute photon emission intensities of ^{103m}Rh. The procedure includes activity measurement using a primary method, liquid scintillation, and photon emission intensity measurement using X-ray spectrometry, on the same sample.

5.2.1 Source preparation

Due to the short half-life of ^{103m}Rh, a specific irradiation was conducted at the nuclear reactor ISIS (CEA Saclay), immediately before chemical preparation of the samples for measurements. The dissolution of pure rhodium is very complex and difficult to obtain in the laboratory. For this experiment the sample consist in a rhodium(III) chloride powder, with the formula $RhCl_3(H_2O)_n$. The $RhCl_3$ was irradiated in the reactor core, placed in a thermal neutron filter to avoid activating chlorine. The powder is soluble in water and allowed having samples quickly ready for measurements in liquid scintillation and spectrometry.

5.2.2 Activity measurement

The activity measurement was performed by liquid scintillation (LS), using the triple-to-double coincidence ratio method (TDCR). After dissolution, the rhodium source is mixed with a commercial liquid scintillator and the scintillating sources are measured using a triple photomultiplier LS counter. The detection efficiency is deduced from the triple to double coincidence ratio, using a model describing the light emitted by the source, from the radiation-matter interaction to the statistics of the light emission. This method is described in detail in reference [14]. The uncertainty of the activity is evaluated with a Monte Carlo method, following the recommendations of [15].

5.2.3 Photon emission intensity measurement

In parallel, X-ray spectrometry allows to determine photon emission intensities. A specific container was optimized for measuring low-energy X-rays. It was filled with the radioactive solution and placed at the reference distance. The efficiency calibration curve required corrective factors to take into account the geometry difference between a point source and the volume source. These corrections can be obtained by Monte Carlo method. Accurate processing of the X-ray spectra requires deconvolution of the K X-ray lines with peak shape taking into account scattering effect (low-energy tailing). The results are under processing but it is expected to derive photon emission intensities with relative combined standard uncertainties around 3%.

6 Self-fluorescence corrections

In this section we focus on the additional fluorescence induced in niobium dosimeters. The typical composition of niobium foils used for dosimetry includes other elements (Table 1). The quantities were determined by mass spectrometry or by neutron activation method (Ta). These impurities are activated during irradiation in the reactor. For example, ^{182}Ta is activated by radiative capture from ^{181}Ta, ^{181}Ta(n,γ)^{182}Ta. In addition, other radioactive isotopes of Nb are created, such as ^{92}Nb and ^{94}Nb by ^{93}Nb(n,2n)^{92}Nb and ^{93}Nb(n,γ)^{94}Nb reactions. After irradiation, some of these impurities are still present during measurements, because of their half-lives, and can be troublesome: ^{94}Nb, ^{95}Nb, ^{92m}Nb and ^{182}Ta.

Table 1. Impurities present in niobium dosimeters

Elements	Quantities (ppm)
Mo	14
W	12
Ta	4.6
Zr	2
Fe	0.06
Ni	0.02
Cr	0.004
Co	0.0003

Moreover, the presence of ^{60}Co has been occasionally observed during measurement. Photons and electrons originating from the decay of these impurities (blue arrow on Figure 6) can interact with atoms of the dosimeter itself by photoelectric effect or other electromagnetic interactions. The dosimeter material is ionised, and photo-electrons are thus ejected from atoms of niobium. This is followed by electron rearrangement, with X-rays emission of niobium. This fluorescence effect generates an extra niobium X-ray emission (red arrows on Figure 6) which is added to the one due to the decay of ^{93m}Nb (green arrows on Figure 6). Consequently, this increase of the number of counts under the full-energy peaks of ^{93m}Nb leads to an overestimation of the dosimeter activity and corrective factors and must be taken into account to derive the activity of ^{93m}Nb only.
The self-fluorescence coefficients were calculated analytically in 1972 (Table 2) for ^{182}Ta, ^{94}Nb, ^{95}Nb and ^{92m}Nb. The coefficients are expressed in $s^{-1}.Bq^{-1}$, indicating the number of fluorescence X-rays emitted per second and per decay of the impurity.

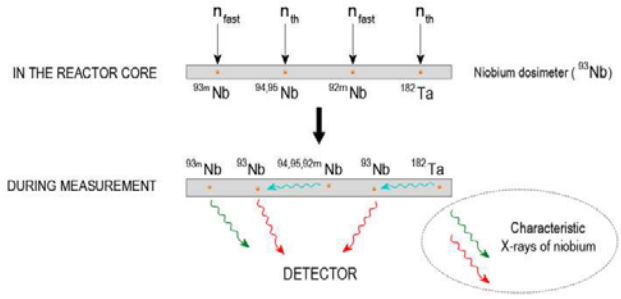

Fig. 6. Scheme of the self-fluorescence in a niobium dosimeter

However, they were calculated only for main energy lines and did not take into account the electrons (or positron) interactions for ^{182}Ta and ^{92m}Nb and the self-absorption of Nb X-rays in the dosimeter following the electronic rearrangement [16]. It was thus decided to actualize the contributions of the impurities in the dosimeters spectra using Monte Carlo method.

7 Monte Carlo method and results

7.1 GEANT4 simulation

The assessment of the coefficients for all radionuclides mentioned above requires simulating radioactive decay according to the decay scheme for each radionuclide. This means taking into account the branching ratios, electronic and photonic emission intensities and their interactions with matter and atomic relaxation processes. GEANT4 enables to simulate radioactive decay thanks to the module "*G4RadioactiveDecay*" and its associated classes. Instead of decay data taken from ENSDF files [17], we preferred to use, when they were available, decay data recommended by the Decay Data Evaluation Project (DDEP) and published by the LNHB [18]. For ^{94}Nb and ^{92m}Nb, we took ENSDF data. Thus we used PENNUC code, which simulate random decay pathways of radioactive nuclides, and associated decay data files [19]. PENNUC generates file a called "CASCADE" which is then read by GEANT4, simulating radioactive decay while taking into account the branching ratios, emission intensities (for electrons, photons and positrons) and internal conversion with recommended data. The electromagnetic physics used in the GEANT4 simulation is the physics models of PENELOPE for electrons, positrons and photons, which is dedicated to the low-energy interactions (Atomic effects, fluorescence, Doppler broadening …).
The geometry of the simulation is the same as for efficiency calculation, but the source is not a point but a niobium volume with the same dimensions as those of dosimeters under study. The particles (photons, electrons and positrons) are emitted inside the niobium volume with a random starting position and a random direction within a solid angle of 4π steradian.
The energy of any particles deposited in the detector volume, is recorded in a root file. The result is an energy spectrum from which the self-fluorescence coefficient is calculated for a given impurity. This coefficient is obtain with the following formula

$$C_{N,X} = \frac{\sum_i N_{X_i}}{N_D} \frac{1}{\varepsilon_X} \quad (5)$$

Where "$C_{N,X}$" is self-fluorescence coefficient for the radionuclide "N" (N = ^{182}Ta, ^{95}Nb…) and the specific characteristic X-ray "X" (X = Kα or Kβ), "N_{Xi}" is the number of counts under the full-energy peak for the line "X_i" (i = *[1, 2]* for Kα or i = *[1, 5]* for Kβ), "N_D" is the number of simulated decay and "ε_X" is the efficiency for the mean energy of the line "X". The total coefficient "C_N" for a radionuclide is simply the addition of the "$C_{N,K\alpha}$" and "$C_{N,K\beta}$" coefficient values.
Simultaneously, we count the number of photons exiting the niobium volume by discriminating the type of the particle, its energy and the process responsible of the ionisation of the niobium atom: "photo-electric effect", "electron ionisation" and "Compton scattering". Thus, it is possible to determine the particles at the origin of the atom ionization and subsequent fluorescence emission:

electrons for "electron ionisation" or photons for "photo-electric effect" or "Compton scattering".

7.2 Results and discussion

The coefficients were calculated from the spectra obtained by the simulations for the niobium energy lines. The treatment of the spectra is quite simple since full-energy peaks appear as Dirac functions from which the background was subtracted. The background comes from the energy deposited indirectly by electrons (Bremsstrahlung) and Compton scattering. The coefficients values were obtained from simulations with several decays for each radionuclide. Table 2 shows the results obtained, with standard uncertainties calculated according to the GUM [15], and compares them with the coefficients assessed in 1972. These results are valid only for a solid angle less or equal to the one of the geometry in the simulation.
For ^{182}Ta, both recent and former values are rather close, although values in 1972 did not take into account electron interactions and self-absorption of Nb fluorescence X-rays in the dosimeter. By tracking the origin of the fluorescence of niobium as explained above, we can determine the ratio of X-rays number resulting from the electron interactions in the dosimeter on the total number of fluorescence X-rays. For this impurity, twenty percent of the X-ray fluorescence is due to electrons. The other part is due to the photoelectric and Compton effects.

Table 2. Comparison between coefficients obtained in this work and coefficients calculated in 1972.

Impurity	Our work ($s^{-1}.Bq^{-1}$)	In 1972	Relative difference
^{92m}Nb	0.00067 (4)	0.021	> 3000%
^{94}Nb	0.0119 (2)	0.0055	54%
^{95}Nb	0.00310 (6)	0.0033	11.1%
^{182}Ta	0.0645 (6)	0.077	19.4%
^{60}Co	0.00821 (11)	-	-

As for ^{182}Ta, both recent and former values for ^{95}Nb agree quite well. In 1972 they tried to take into account interactions of electrons coming from the β^- decay [16]. They checked their calculations experimentally, and were able to find a value reasonably good. In addition, knowledge on the decay scheme and data has not changed significantly since 1972, whether on the beta spectrum, the half-life, etc.
For ^{94}Nb, both recent and former values differ by a factor two. As for ^{95}Nb, they tried to take into account in 1972 interactions of electrons and evaluated experimentally their calculations. But, knowledge on the decay scheme and data changed significantly since 1972, especially data on the beta spectrum. For example, the maximum energy of the spectrum has decreased from 610 keV in 1972 to 470 keV today. For these two radionuclides, the contribution of the electrons to the fluorescence emission is higher than eighty percent. The consideration of their interactions is essential, however the theoretical calculation and experimental validation is very complex especially with the calculation means available at the time.
For ^{92m}Nb, both recent and former values disagree by a factor upper than thirty. In 1972, they deduced the coefficient by observing the evolution of the ratio of Zr X-rays Nb peaks [16]: ^{92m}Nb disintegrates to ^{92}Zr and emits Zr X-rays. They have probably considered that the radionuclide is only emitting Zr X-rays in the dosimeter, although this may not be the case.
The magnitude of corrections on the dosimeter activity for each impurity depends on the activity of this impurity. However we notice that the ^{182}Ta and ^{94}Nb can be troublesome if a significant activity is observed relatively to ^{93m}Nb activity. For ^{92m}Nb, the impact is quite negligible, especially since it is generally observed with low activities.

Conclusion

Low-energy X-ray spectrometry applied to activity measurement of solid dosimeters is challenging. Different aspects have been examined in the present study and different experiments have been conducted to improve the atomic data of rhodium and niobium, as well as the decay scheme of ^{103m}Rh. The importance of corrective factors has been underlined and Monte Carlo simulation has been used to compute self-absorption and fluorescence effects. The use of Monte Carlo method enables more accurate calculations of the self-fluorescence corrections than previously. Moreover, modern particle transport codes make possible to take into account all the effects occurring at low energies and to clearly identify the main ones. Due to the present study, significant improvement in the measurement methodology for solid dosimeters is expected.

The authors would like to thanks H. Carcreff and O. Vigneau (CEA-DEN) for their valuable assistance and support in the Rh irradiation experiment.

References

1. A. Ballesteros, L. Debarberis, W. Voorbraak, J. Wagemans, P. D'hondt, Prog. Nucl. Energy **52**, 615-619 (2010)
2. W. P. Voorbraak, T. Kekki, T. Serén, M. van Boxstaele, J. Wagemans, J.R.W. Woittiez, *Proceeding of the FISA-2003 Conference* (2003), https://cordis.europa.eu/fp5-euratom/src/ev-fisa2003.htm
3. V. Sergeyeva, C. Domergue, C. Destouches, J.-M. Girard, H. Philibert, D. Beretz, J. Bonora, N. Thiollay, A. Lyoussi, EPJ Web Conf. **106**, (2016) DOI: http://dx.doi.org/10.1051/epjconf/201610605011
4. C. Domergue, D. Beretz, C. Destouches, J.-M. Girard, H. Philibert, J. Plagnard, *Advancements in*

Nuclear Instrumentation Measurement Methods and their Applications (ANIMMA), 2009 First International Conference on, 1-6 (2009) DOI: 10.1109/ANIMMA.2009.5503820
5. M.-M. Bé, V. Chisté, C. Dulieu, M.A. Kellett, X. Mougeot, A. Arinc, V.P. Chechev, N.K. Kuzmenko, T. Kibédi, A. Luca, A.L. Nichols. *Table of Radionuclides*, *Monographie BIPM-5* **8** (BIPM, Pavillon de Breteuil, F-92310 Sèvres, France, 2016)
6. *Private Communication*. M.-M. Bé, M.A. Kellett (2016)
7. F. Salvat, *PENELOPE-2014: A Code System for Monte Carlo Simulation of Electron and Photon Transport* (OECD/NEA Data Bank, Issy-les-Moulineaux, France, 2015)
8. S. Agostinelli et al., Nucl. Instrum. Methods Phys. Res., Sect. A **506**, 250-303 (2003)
9. M.-M. Bé, *Table of Radionuclides – Introduction* (Technical report, CEA, LIST, LNE-LNHB, 2011)
10. J. Riffaud, M.-C. Lépy, Y. Ménesguen, A. Novikova, X-Ray Spectrom. (to be published)
11. Soleil synchrotron (2007), http://www.synchrotron-soleil.fr/portal/page/portal/Accueil
12. Y. Ménesguen, M.-C. Lépy, Nuc. Instrum. Methods Phys. Res., Sect. B **268**, 2477-2486 (2010)
13. Y. Ménesguen, M. Gerlach, B. Pollakowski, R. Unterumsberger, M. Haschke, B. Beckhoff, M.-C. Lépy, Metrologia **53**, 7-17 (2016)
14. P. Cassette, M.-M. Bé, F. Jaubert, M.-C. Lépy, Appl. Radiat. Isot. **60**, 439-445 (2004)
15. JCGM, *Evaluation of measurement data - Supplement 1 to the "Guide to the expression of uncertainty in measurement" - Propagation of distributions using a Monte Carlo method* (BIPM, 2008)
16. R. Lloret, *Utilisation du niobium comme intégrateur de fluences élevées de neutrons rapides* (Technical report, CEA-CEN/G-Service des piles, 1973)
17. Chapter 44, *Geant4 Physics Reference Manual* (2015)
18. M.A. Kellett, EPJ Web Conf. (to be published)
19. E. Garcia-Torano, V. Peyres, M.-M. Bé, C. Dulieu, M.-C. Lépy, F. Salvat, Nuc. Instrum. Methods Phys. Res., Sect. B (to be published)